SPACE TELESCOPE SCIENCE INSTITUTE
Operated for NASA by AURA

Instrument Science Report WFC3 2007-24

WFC3 TV2 Testing: UVIS Filtered Throughput

Thomas M. Brown
Oct 25, 2007

ABSTRACT

During the most recent WFC3 thermal vacuum (TV) testing campaign, several tests were executed to measure the UVIS channel throughput through its filters. These tests complement the tests of the UVIS channel system throughput, which is done without a filter in the beam. The UVIS filter transmissions were already well-characterized by scans of the filters at JPL and GSFC, so the filtered tests here are geared toward verification instead of characterization. Each of the filters was checked at a single in-band wavelength, showing good agreement with previous scans. Additional tests checked the red leak performance in several UV filters, and the red end cutoff of the F850LP, which is determined by the detector instead of the filter. The red leak checks at 450 nm and 600 nm in the F343N and F336W filters failed, likely due to scattered light in the single monochromator mode of the optical stimulus, but this should be verified in the next TV campaign.

Background

The Wide Field Camera 3 (WFC3) recently underwent ground testing under thermal vacuum (TV) conditions. A spare UVIS detector (UVIS-2) is currently installed in the instrument, replacing the detector in use during the 2004 TV tests (UVIS-1). Among the tests performed in TV is a measurement of the UVIS filtered throughput. The UVIS system throughput in the "CLEAR" mode was measured separately (Brown 2007, ISR WFC3 2007-20), and so the filtered throughput tests are intended to verify the transmission data for the UVIS filters in isolation. These filters were already well-characterized by ground tests at both JPL and GSFC, and it would be impractical to obtain a high-resolution scan of each UVIS bandpass under TV conditions, due to time constraints. These tests thus check a single in-band wavelength for each filter, spot check a few out-of-band wavelengths for the UV filters, and scan the red end cutoff of the F850LP (a bandpass shaped by the detector response). The methodology is very similar to that used in the

UVIS system throughput tests (Brown 2007, ISR WFC3 2007-20), to which the reader is referred for details.

In-Band Transmissions

As done in the UVIS system throughput tests, a 200-micron fiber from the optical stimulus (a.k.a. "CASTLE") provided flux-calibrated illumination of an extended spot on the detector, with a roughly flat top approximately 20 pixels wide and a taper several pixels beyond that. The wide spot allows an average over pixel-to-pixel response and also enables the collection of many counts (>1,000,000) without saturating the detector. The detector was read with an 800x800 subarray on chip 2 of the UVIS detector in the same location used for the UVIS system throughput tests (with the exception of the quad filters), and then aperture photometry was used to measure the count rate, with a radius of 40 pixels and a sky annulus of radii 50-70 pixels. Given the large number of counts in the source and the extremely low background, the use of this large aperture gives the throughput in the equivalent of an "infinite" aperture without introducing unnecessary noise in the measurement. The ratio of measured count rate (electrons/sec) to input CASTLE flux (photons/sec) gives the throughput.

In the CLEAR system throughput tests, the CASTLE was scanned across the entire UVIS channel wavelength range, with two WFC3 exposures at each wavelength and no WFC3 filter in the beam. A single CASTLE flux calibration was performed for each pair of exposures, but the CLEAR throughputs in each pair agreed to much better than 1%, indicating CASTLE and WFC3 stability. In the current tests, there are two WFC3 exposures at each wavelength, but one employs a UVIS filter and one uses the CLEAR mode; each has its own CASTLE flux calibration. We divide the filtered throughput by the clear throughput to obtain the throughput of the filter in isolation, which is then compared to the expected throughput. Both the measured and expected throughput are not at a single wavelength, but instead are calculated as the weighted average in that vicinity, with the nearly monochromatic CASTLE spectrum as the weighting function.

The CASTLE lamps cannot provide an infinitely monochromatic source. With the double monochromator, users can specify a bandpass of 1-13 nm, and the transmission of the double monochromator is shaped like a triangle with a FWHM of the selected bandpass. E.g., a 10 nm bandpass produces a triangle with a base of 20 nm and a FWHM of 10 nm. Thus, what is measured in this test is a weighted average of the transmission in each filter, where this triangular spectrum is the weighting function; we are not measuring the transmission at a single wavelength. This distinction is unimportant for the medium-band (M), wide-band (W), or long-pass (LP) filters, but it is important for the narrow-band (N) filters, because some have a FWHM of only a few nm. The CASTLE bandpass was set to 10 nm for nearly all medium-band, wide-band, and long-pass filters, with the exception of F845M, F814W, and F850LP, where it was 12 nm. The CASTLE bandpass was also set to 10 nm for all of the narrow-band filters. The N-band test procedure was the matter of some debate during the preparation for this TV campaign, because at any setting of the CASTLE bandpass width, the width of the spectrum produced will be a non-negligible fraction of the WFC3 filter bandpass. Thus the spectrum-weighted average of the filter transmission will be very sensitive to any systematic errors in the CASTLE wave-

length calibration and any deviations from a triangular spectrum. The tests of the N-band filters are thus intended as a crude transmission check, to make sure there has not been a catastrophic failure of a coating or other gross problem. No obvious improvement on the procedure arose as part of the TV campaign.

The results of the M, W, and LP filter measurements are shown in Table 1, while the results of the quad (mostly N but also one M) and N filters are shown in Table 2. Some of the filters in Table 1 were tested two to three times, and in those cases the results have been averaged, although the distinct measurements generally agreed to better than 1% and always better than 3%. All of the filters in Table 1, except one (F775W), agreed with expectations at the 4% level or better. The F775W transmission was 16% higher than expected, and this is consistent with the tests of this filter in the 2004 TV campaign (Brown & Reid 2005, ISR WFC3 2005-02). In the previous TV campaign, the F218W and F225W filters had lower-than-expected transmission, but those filters were replaced, and the new filters show good agreement with expectations. All of the filters in Table 2 agree with expectations to better than 10%; as stated above, the tests of the N bands are really meant as a gross verification, given the systematics introduced by the finite CASTLE bandpass and the narrowness of the N-band filters. It is worth stressing that the N-band transmissions are a spectrum-weighted average over the CASTLE bandpass, not the peak transmission of the filter.

Table 1: Throughput results for M, W, and LP filters

filter	wavelength (nm)	transmission	transmission relative to the expected value
F200LP	300	0.989	1.003
F218W	218	0.196	0.984
F225W	225	0.314	1.008
F275W	275	0.373	0.994
F300X	300	0.365	1.028
F336W	336	0.763	1.037
F350LP	555	0.983	1.008
F390M	390	0.846	1.014
F390W	390	0.934	0.987
F410M	410	0.888	0.984
F438W	438	0.819	1.013
F467M	467	0.895	1.001
F475W	475	0.884	1.001
F475X	475	0.925	0.996
F547M	547	0.842	1.015
F555W	555	0.871	1.000
F600LP	642	1.003	1.026
F606W	606	0.961	1.003
F621M	621	0.968	1.013
F625W	625	0.892	0.991
F689M	689	0.912	1.007
F763M	763	0.969	1.016
F775W	775	0.965	1.159
F814W	814	0.944	0.991
F845M	845	0.950	0.998
F850LP	880	0.876	1.034

Table 2: Throughput results for quad and N-band filters

filter	wavelength (nm)	transmission	transmission relative to the expected value
F280N	280	0.089	0.933
F343N	343	0.701	1.019
F373N	373	0.321	0.942
F395N	395	0.524	0.929
F469N	469	0.294	0.989
F487N	487	0.400	0.925
F502N	502	0.449	0.975
F631N	630	0.396	0.936
F645N	645	0.529	0.950
F656N	656	0.132	0.920
F657N	657	0.716	0.978
F658N	658	0.217	0.926
F665N	665	0.753	0.965
F673N	676	0.688	0.929
F680N	688	0.928	0.985
F953N	953	0.629	0.979
FQ232N	233	0.034	1.014
FQ243N	242	0.049	1.009
FQ378N	379	0.570	0.935
FQ387N	387	0.202	0.923
FQ422M	422	0.493	0.948
FQ436N	436	0.243	0.946
FQ437N	437	0.182	0.939
FQ492N	493	0.642	0.934
FQ508N	509	0.731	0.975
FQ575N	575	0.126	0.917
FQ619N	620	0.431	0.960
FQ634N	635	0.448	0.961
FQ672N	671	0.157	0.959
FQ674N	673	0.106	0.929
FQ727N	727	0.436	0.929
FQ750N	750	0.446	0.915
FQ889N	889	0.626	0.977
FQ906N	906	0.601	0.922
FQ924N	924	0.628	0.988
FQ937N	937	0.616	0.982

Red End of the F850LP Bandpass

As stated earlier, the F850LP bandpass is limited on the red end by the response of the detector. A separate throughput test was thus run with F850LP, stepping in wavelength on a fine grid with a 12 nm bandpass on the CASTLE. The goal here was different than the tests in the previous section. Detailed scans of the transmission of each filter have already been obtained from GSFC and JPL, and the tests in the previous section were intended to verify those transmission curves at a single wavelength in each filter, by dividing the filtered throughput by the CLEAR throughput to obtain the filter transmission. The F850LP transmission data extend to 1100 nm, but the F850LP throughput is the product of the filter transmission, the UVIS channel optics, and the CCD QE, most of which were not characterized beyond 1000 nm. Thus, the point of the tests described here was to obtain the total F850LP throughput at the red end of its range (not verify the filter transmission data). The test was repeated on each chip of the detector, to provide a measure of the red-end throughput for each chip in this filter. Because some of the component measurements do not extend beyond 1000 nn, there is no model of the F850LP beyond that point. The results are shown in Table 3. The chips exhibit a similar throughput from 850 to 1100 nm, with all deviations at the 10% level or less. The agreement with the expected throughput is poor, as found with the UVIS system throughput (CLEAR) in this TV campaign (Brown 2007, ISR WFC3 2007-20), presumably due to systematic errors in the component measurements at the end of the UVIS range.

In addition to the throughput measurements of the 200 micron spot, we also performed a series of exposures with flat-field illumination at the same wavelengths and bandpass settings on CASTLE. At the short end of this wavelength range, the flat field shows the usual diamond-shaped pattern, due to the glint on the UVIS detector and the CCD window ghosts (Figure 1; see also Brown 2007, ISR WFC3 2007-21). At longer wavelengths, CCD fringing becomes obvious (Figure 2), and by the red end of the wavelength range, the silicon becomes relatively transparent, such that one can see the glue used to adhere the detector to its package (Figure 3; P. McCullough, private communication). It is thus worth stressing that the throughput measured here is only for two field points (one on each chip), and that actual science observations will require a significant flat field correction when observing objects with strong emission lines in the F850LP range.

Table 3: Throughput measurements of the F850LP filter

wave-length (nm)	chip 1 obs. count rate (e^-/s)	chip 1 throughput	chip 1 throughput relative to expected	chip 2 obs. count rate (e^-/s)	chip 2 throughput	chip 2 throughput relative to expected
850	85317	9.68E-02	1.162	84182	9.47E-02	1.145
890	44405	1.50E-01	0.847	42529	1.44E-01	0.841
910	63345	1.37E-01	0.813	59798	1.30E-01	0.801
930	72067	1.13E-01	0.758	68893	1.09E-01	0.762
950	81074	9.11E-02	0.724	78649	8.84E-02	0.742
970	84430	6.54E-02	0.655	83702	6.50E-02	0.676
980	85321	5.56E-02	0.647	86083	5.62E-02	0.671
990	82128	4.62E-02	0.654	81857	4.60E-02	0.656
1000	73666	3.60E-02	1.128	74044	3.61E-02	1.121
1010	64220	2.69E-02	N/A	62766	2.62E-02	N/A
1020	52990	1.96E-02	N/A	51833	1.93E-02	N/A
1030	41761	1.38E-02	N/A	41351	1.37E-02	N/A
1040	29626	8.83E-03	N/A	30013	8.98E-03	N/A
1050	22674	6.22E-03	N/A	23164	6.36E-03	N/A
1060	17560	4.45E-03	N/A	17494	4.45E-03	N/A
1070	14624	3.48E-03	N/A	13874	3.31E-03	N/A
1080	10066	2.28E-03	N/A	11161	2.53E-03	N/A
1090	7652	1.64E-03	N/A	7462	1.61E-03	N/A
1100	6655	1.35E-03	N/A	6307	1.28E-03	N/A

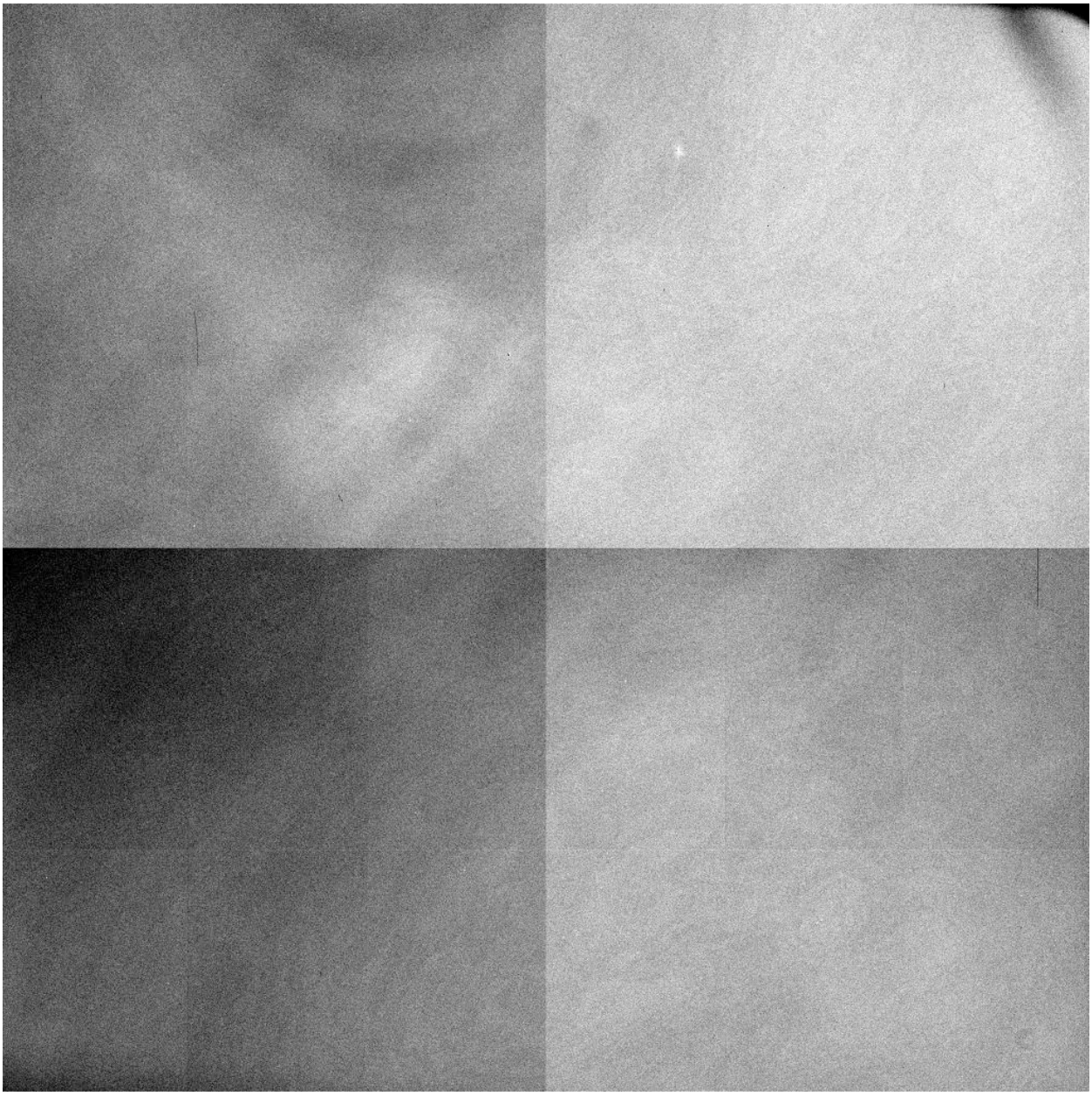

Figure 1: An F850LP flat-field image with monochromatic illumination at 850 nm shows the usual diamond-shaped pattern seen in UVIS flat field images. This pattern is obvious in the upper left-hand quadrant, while the other half of the diamond, in the lower right-hand quadrant, is somewhat difficult to see at this stretch.

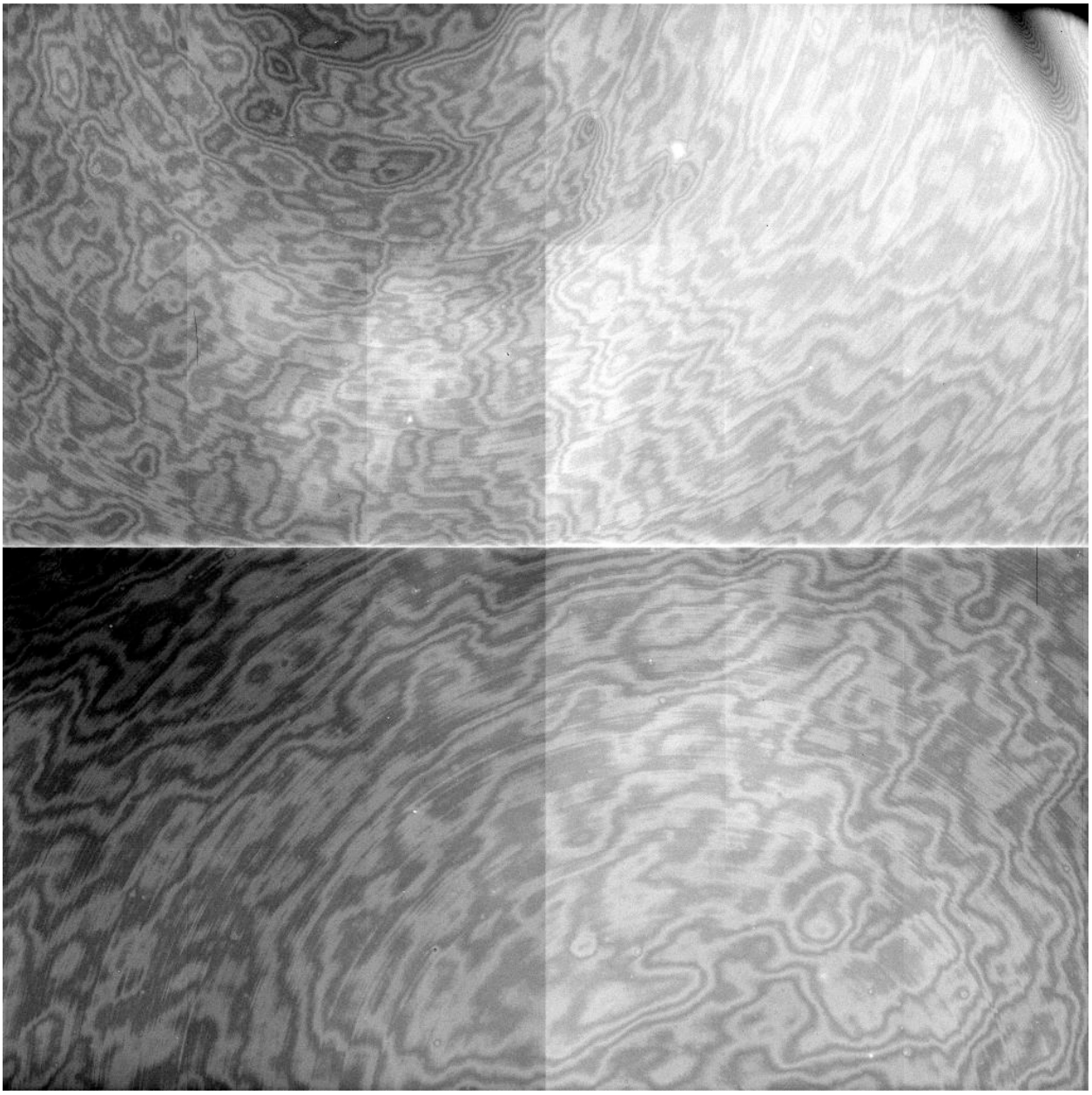

Figure 2: The same as in Figure 1, but at 990 nm, showing strong fringing. The brighter bands are roughly 5% brighter than the darker bands.

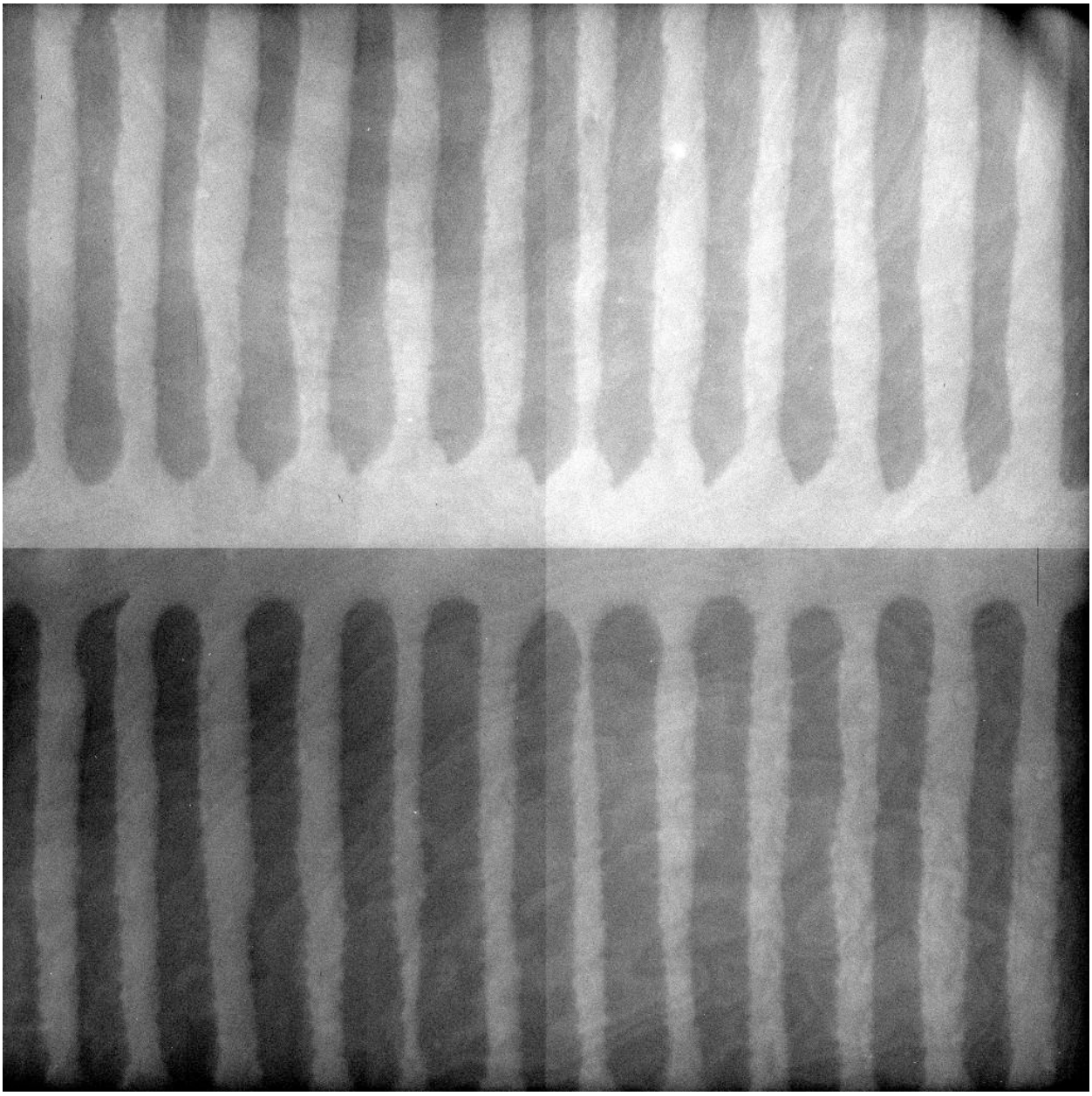

Figure 3: The same as in Figure 1, but at 1100 nm. The silicon is becoming relatively transparent at these wavelengths, so that the glue adhering the detector to its package becomes visible (P. McCullough, private communication). The brighter regions of this "rib cage" pattern are roughly 10% brighter than the dark regions.

Red leaks in the UV Filters

In addition to an in-band measurement of the throughput in each filter, we also obtained out-of-band measurements of some UV filters (F218W, F225W, FQ232N, FQ243N, F275W, F280N, F336W, and F343N) at four wavelengths: 450, 600, 750, and 900 nm. These were configured in a similar manner as the in-band exposures, except that the single monochromator on the CASTLE was used, with a bandpass of 125 nm. All but FQ243N were observed in the nominal filtered throughput location (in the middle of the lower left-hand quadrant, on chip 2); FQ243N was observed in the middle of the lower right-hand quadrant, on chip 2. In the single monochromator mode, the transmission of the CASTLE monochromator is roughly flat-topped over the bandpass specified (instead of the triangular transmission produced in double monochromator mode). This test is thus measuring the weighted average of the throughput over this wide bandpass, where the weighting function is the product of the monochromator transmission (a roughly flat-topped function) and the Xenon lamp spectrum (which includes both a bright continuum and a series of emission lines). The calculation for the expected average transmission does not account for the lamp spectrum, and instead assumes a flat distribution with wavelength; thus, we do not expect perfect agreement between measurement and expectations. The test is only a rough check of the red leak for these filters. The results are shown in Table 4. Overall, the agreement is good, given the caveats. However, there are a couple of problems.

One problem was that the 450 nm and 600 nm images were grossly saturated in the F336W and F343N filters, such that no measurement of the throughput could be made for these filters at these wavelengths. At first glance, it was not obvious how the images could have saturated (see Figure 4). The CASTLE spectrum at 450 nm includes the red edge of the in-band transmission for both F336W and F343N, but the average transmission over the 125 nm span is still 3 orders of magnitude lower in F336W and F343N than it is in F280N, and the F280N image looked fine at this wavelength. The same CASTLE configuration was used for a filter sequence F275W-F280N-F336W-F343N at each wavelength. If CASTLE was misconfigured, one would expect the F275W and F280N images to show saturation, too. If the F336W or F343N filters had a pinhole, one would expect to saturate at 750 nm and 900 nm, too, and that did not happen; furthermore, flat field images of these filters show no problems at 600 nm. In addition, the 600 nm throughput exposures span regions of the F336W and F343N filter curves with very low, nearly flat transmission. The best explanation (G. Hartig & R. Telfer, private communication) is scattered light in the CASTLE monochromator. The CASTLE single monochromator mode can produce significant scattered light at wavelengths outside of the nominal bandpass; this light is very well suppressed in the double monochromator mode. It is likely that the scattered light in the 450 nm and 600 nm exposures is falling in-band for the F336W and F343N filters but not the F275W and F280N filters. Additional spot checks of the F336W and F343N filter transmission at a few wavelengths (e.g., 450, 500, 600, & 650 nm) should be performed in the next TV campaign, using the double monochromator, to make sure this explanation is correct.

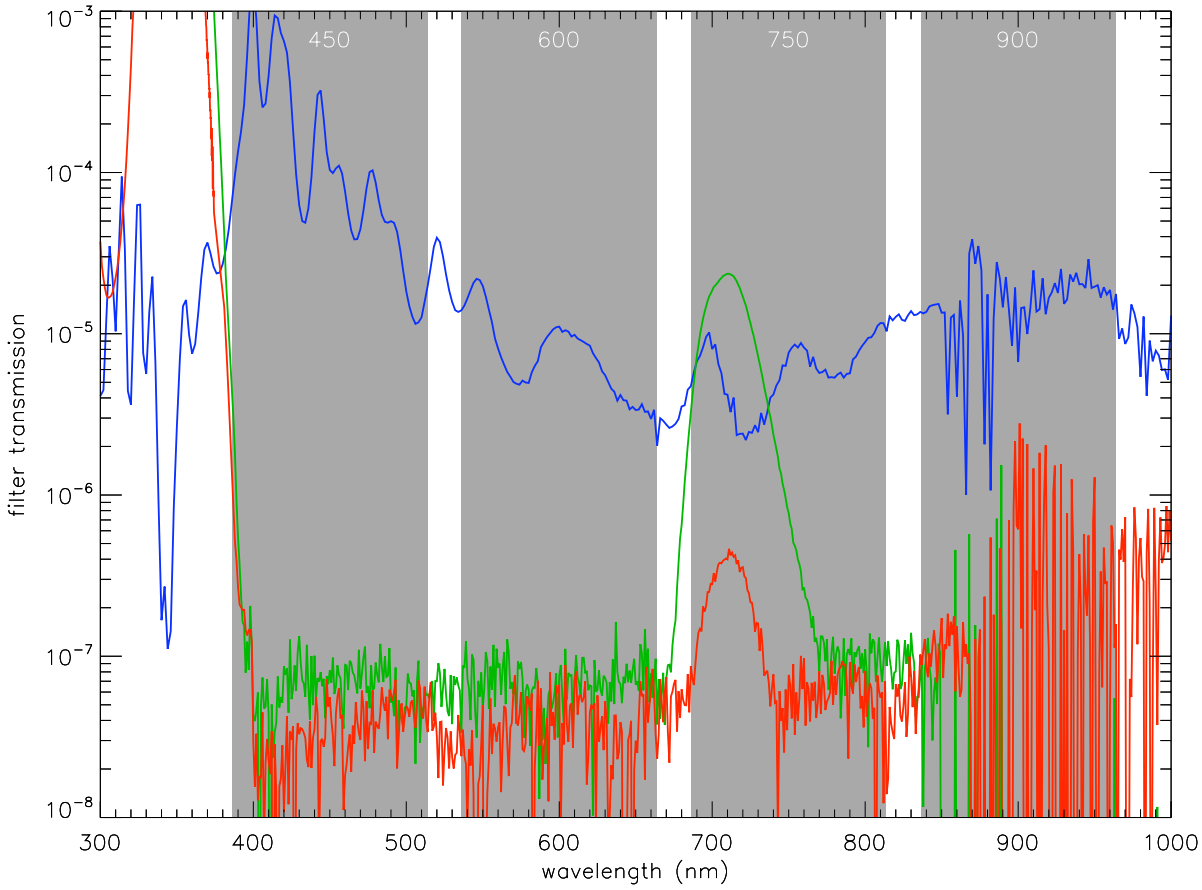

Figure 4: The transmission of the F280N (*blue*), F336W (*green*), and F343N (*red*) filters, with the 4 wavelength regions used for red leak checks shown (*grey*). The F336W and F343N images at 450 nm and 600 nm were grossly saturated (so that no throughput could be measured), but the F280N image obtained with the same CASTLE configuration was not. The F336W and F343N images at 750 nm and 900 nm were not saturated, either.

In addition to the illumination with a 200 micron fiber, we also illuminated with a flat-field image at 600 nm, to see if the point used for the throughput measurements is representative of the field as a whole. Both FQ232N and FQ243N are known to have unpainted pinholes, and these create large donuts in the flat field images (approximately 1000 pixels in diameter), because the filters are out of focus for external illumination. The FQ232N flat field image implies that the throughput point is representative of that quadrant, but the FQ243N flat field image implies that the throughput point is subject to illumination from the pinhole (Figure 5); specifically, the flat field illumination is roughly twice as bright in the vicinity of the throughput measurement, compared to the darker regions of the flat field image. In the next TV campaign, it would be good to move the FQ243N throughput measurements to a point further from the quadrant center, toward the lower right-hand corner of the detector.

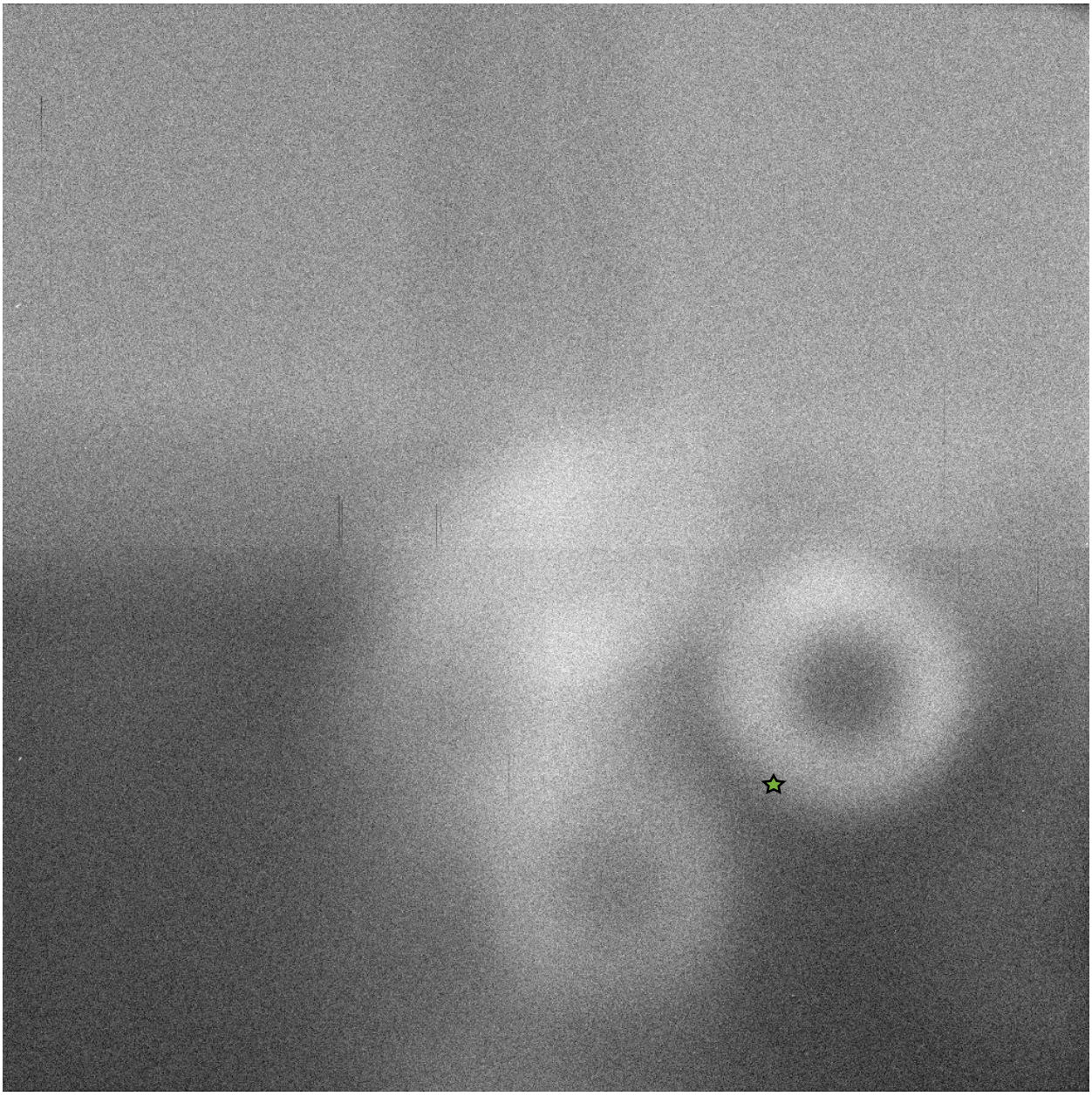

Figure 5: The flat-field image at 600 nm for the FQ243N (quad) filter, with donuts from out-of-focus pinholes in the filter. The approximate location of the spot used for the FQ243N throughput measurement is indicated (*green star*). At this location, the flat-field image is roughly twice as bright as it is in the darker region immediately below the donut.

Table 4: Red leak measurements in the UV filters

filter	wavelength (nm)	exp. time (s)	observed count rate (e-/s)	throughput	throughput relative to expected
F218W	450	1	1929274	2.55E-05	1.126
F225W	450	2	361489	4.78E-06	1.166
FQ232N	450	1	1072797	1.42E-05	1.263
FQ243N	450	1	1516438	2.00E-05	1.613
F275W	450	1	506726	6.70E-06	0.994
F280N	450	1	6886701	9.10E-05	1.092
F336W	450	140	saturated	N/A	N/A
F343N	450	240	saturated	N/A	N/A
F218W	600	20	27697	5.30E-07	1.314
F225W	600	3	116294	2.23E-06	0.95
FQ232N	600	2	166474	3.19E-06	0.619
FQ243N	600	3	176435	3.38E-06	1.109
F275W	600	5	74453	1.43E-06	1.195
F280N	600	2	236289	4.52E-06	1.284
F336W	600	210	saturated	N/A	N/A
F343N	600	290	saturated	N/A	N/A
F218W	750	40	7996	1.96E-07	0.877
F225W	750	6	97228	2.38E-06	0.984
FQ232N	750	3	100337	2.45E-06	0.652
FQ243N	750	4	121445	2.97E-06	1.01
F275W	750	12	36563	8.94E-07	0.852
F280N	750	5	82011	2.01E-06	0.991
F336W	750	40	70808	1.73E-06	0.781
F343N	750	660	984	2.41E-08	0.499
F218W	900	2	115143	2.48E-07	0.535
F225W	900	1	1273931	2.75E-06	0.749
FQ232N	900	1	1278374	2.76E-06	0.831
FQ243N	900	1	1200658	2.59E-06	1.161
F275W	900	1	545398	1.18E-06	0.939
F280N	900	1	1019806	2.20E-06	0.743
F336W	900	370	764	1.65E-09	0.221
F343N	900	5	475	1.03E-09	0.02